Ionization of the He, Ne, Ar, Kr, and Xe isoelectronic series by proton impact

J. E. Miraglia and M. S. Gravielle
Instituto de Astronomía y Física del Espacio, Consejo Nacional de Investigaciones Científicas y Técnicas and Departamento de Física, Facultad de Ciencias Exactas y Naturales, Universidad de Buenos Aires, Casilla de Correo 67, Sucursal 28, C1428EGA Buenos Aires, Argentina
(Received 4 September 2008; published 6 November 2008)

In this paper we report ionization cross sections of positive Li^+, Na^+, K^+, Rb^+, neutral He, Ne, Ar, Kr, Xe, and negative F^-, Cl^-, Br^-, I^- ions by impact of protons with energies ranging from 25 to 1000 keV. Cross sections of singly charged ions are relevant to the calculation of electron yields in collisions with insulator surfaces. Calculations were performed within the continuum distorted wave–eikonal initial state method using an angular expansion in spherical harmonics and a numerical evaluation of the radial functions corresponding to both the initial (bound) and the final (continuum) states. The first Born approximation was used on an equal footing. We find that this first-order theory holds for proton energies larger than 300 keV. For comparison, we also calculate the shellwise local plasma approximation. Our results show that it gives a good account of the cross sections for neutral targets.

DOI: 10.1103/PhysRevA.78.052705 PACS number(s): 34.50.Fa, 32.80.Aa

I. INTRODUCTION

Collisions of protons with insulator surfaces have become an active research field in recent years. Our particular interest focuses on the electron yield as well as the total energy loss of protons impinging on NaCl-insulator surfaces at grazing angles. In this research field, several experiments have been carried out at relatively high energies, where the electron production reaches 100 electrons per incident proton [1–3]. From the theoretical point of view, one approximation to make the problem tractable is to consider the surface as a grid of independent ions. Thus, the target is considered to be composed of an array of alkali-metal and halide ions situated at places given by the crystal parameters [4]. The trajectory of the projectile is classically calculated, considering the interaction with every single ion of the crystal. In each segment of its trajectory, the projectile collides with the nearest insulator ion, promoting electrons to the continuum (contributing to the yield) and in consequence the projectile slows down (which accounts for its energy loss). The key quantity to be calculated is then the ionization cross section studied in this paper.

The shellwise local plasma approximation (SLPA) has been used to calculate yield and total energy loss of protons colliding with insulator surfaces [4,5]. This model calculates the energy deposited within the dielectric formalism, taking into consideration the electronic density of the region visited by the projectile. The resulting energy loss gives a very good account of all the available experiments but electron yields for protons on KCl and LiF seem to fall short when compared with experiments at high energies [5]. The stopping (i.e., the first moment in the energy loss) as well as the straggling (the second moment) are expected to be well described by the SLPA. These energy moments are determined by head-on collisions which take place at *short* projectile-electron distances. But the cross section (i.e., the zero moment) is mainly described by the low-electron-energy region where the local hypothesis is not appropriate because it involves *large* projectile-electron distances.

On the other hand we have also used the continuum distorted wave–eikonal initial state (CDW-EIS) approximation to calculate electron yields of protons colliding with NaCl-insulator surfaces within the impact parameter treatment [6] but the CDW-EIS approximation employed involved the use of an effective charge to represent the target interaction in the final continuum state. This loss of consistency between the descriptions employed to represent the initial (described by the Hartree-Fock-Slater method) and the final (described by a continuum wave function with an effective Coulomb charge) channels could be considered a questionable point of the theory. Therefore, the state of the investigations requires the calculation of ionization cross sections with a method which can be considered a reliable reference to contrast the SLPA and previous CDW-EIS predictions.

With this aim in mind, in this paper we undertake the task of calculating the ionization cross section with the CDW-EIS approximation, which is perhaps a more—if not the most—reliable approximation within the *independent electron model* in the high-energy range [7]. To avoid doubts we calculate the CDW-EIS matrix element in the most rigorous possible way, i.e., by solving the radial Schrödinger equation for different angular momenta for both: the initial bound and the final continuum states. Thus we can assure the proper description of the continuum wave function and its mathematical orthogonality to the bound state. This calculation is known to be very complicated and lengthy due to the large amount of numerical integrations, but we decided to carry it out to attain solid and unambiguous conclusions. As for singly charged target ions in our range of energies there are no available experiments to contrast with our results, in this work we also report calculations on neutral rare gases for which ionization cross sections were measured. Furthermore, for neutral He, Ne, and Ar gases, we have the advantage that calculations with the full CDW-EIS method were already reported by Gulyás, Fainstein and co-workers [8–11], which let us test the reliability of the potentials used in our numerical procedure. In synthesis, we have calculated the ionization of the He (He^0,Li^+), Ne (F^-,Ne^0,Na^+), Ar (Cl^-,Ar^0,K^+), Kr (Br^-,Kr^0,Rb^+), and Xe (I^-,Xe^0) isoelectronic series.

Since the theoretical expressions involved in the calculation of the Born and CDW-EIS approximations are well established, we will bypass the algebra and concentrate directly on the details of the calculations in the next section. Results and conclusions are presented in Secs. III and IV, respectively. Atomic units are used all along.

II. DETAILS OF THE CALCULATIONS

In general, the methods to calculate T-matrix elements are rather standard. The basic technique consists in expanding both the initial and final wave functions in spherical harmonics times radial wave functions, which require the numerical solution of the radial Schrödinger equation. The integration on the angular variables can be calculated in a closed form with the help of the Clebsch-Gordan coefficients but radial functions need to be integrated numerically using a radial grid. The final expression for the Born approximation can be found in Ref. [12], for example. The CDW-EIS T-matrix element involves not only the usual free-bound element, such as the Born approximation, but also another term including a gradient operator between both states. Using the gradient formula [13] we obtain an expression similar to the one reported by other authors [8]. The CDW-EIS approximation also involves the evaluation of the hypergeometric function ${}_2F_1$, which makes the CDW-EIS calculation far more time consuming than the Born one. The precision and efficiency of the hypergeometric function calculation has always been a matter of concern.

The initial (bound) and final (continuum) radial wave functions were obtained by using the code RADIALF developed by Salvat and co-workers [14]. The number of pivots used to solve the Schrödinger equation ranged between 300 and 1300 points, depending on the number of oscillations of the continuum. The maximum radius of the integration was set around $20\langle r\rangle_{nl}$, $\langle r\rangle_{nl}$ being the mean radius of the initial state. The radial integration was performed using the cubic spline technique. The number of considered angular momenta, $l_{\max}$, varied between 8, at very low ejected-electron energy, up to 24, at the largest energies considered. The same number of azimuth angles were required to obtain a fourfold differential cross section. From 35 to 199 momentum transfers were used to determine a doubly differential cross section. The total cross section was calculated using 20 (fixed) electron angles and from 30 to 48 electron energies, depending on the projectile impact energy. Although the CDW-EIS and Born approximations were calculated on an equal footing, the Born calculation is at least ten times faster. The numerical evaluation of the CDW-EIS cross sections was a very tedious task, which required a large amount of convergence tests and checking to bring the calculation to a reasonable computing time.

A particular strategy was here adopted, which is different from previous schemes. Once obtained, the T-matrix element $T(E,\Omega_E,\vec{\eta})$ for each electron energy (E), electron angle (Ω_E), and projectile transverse momentum transfer $(\vec{\eta})$, it was Fourier expanded as follows:

$$T(E,\Omega_E,\vec{\eta}) = \sum_{m=-l_{\max}}^{l_{\max}} \exp(im\phi_\eta) T_m(E,\Omega_E,\eta), \tag{1}$$

with m the final magnetic number of the spherical harmonic. Terms with $|m|>l_{\max}$ were discarded. In the Born approximation this sum is closed to $l_{\max}$ and so no term is discarded [12]. But for the CDW-EIS approximation this criterion discards higher m terms, which are comparable with the ones *already* neglected in the radial expansion of the corresponding Schrödinger equation. The fourfold differential cross section is then calculated as

$$\frac{d\sigma}{dE\, d\Omega\, d\eta} = \frac{(2\pi)^4}{v^2} \sum_{m=-l_{\max}}^{l_{\max}} |T_m(E,\Omega_E,\eta)|^2, \tag{2}$$

where v is the projectile velocity. Therefore our CDW-EIS results can be considered as a lower limit of the exact element. The ionization cross section from a particular state nlm was calculated with the usual expression $\sigma_{nlm} = \int_0^\infty dE\, \sigma_{nlm}(E)$, $\sigma_{nlm}(E)$ being the singly differential cross section and E the energy of the ejected electron. Total magnitudes, as displayed in this paper, involve the sum over all the relevant states of the target, i.e., $\sigma=\Sigma_{nlm}\sigma_{nlm}$. Except for the He isoelectronic series, the Σ_{nlm} was extended to include two complete shells: i.e., for Ne $(2p_{0\pm1}$, $2s$, and $1s)$, Ar $(3p_{0\pm1}$, $3s$, $2p_{0\pm1}$, and $2s)$, Kr $(4p_{0\pm1}$, $4s$, $3d_{0\pm1\pm2}$, $3p_{0\pm1}$, and $3s)$, and Xe isoelectronic series $(5p_{0\pm1}$, $5s$, $4d_{0\pm1\pm2}$, $4p_{0\pm1}$, and $4s)$.

A. Calculation of the potentials

The central potentials $V_{nl}(r)$ were determined by employing the following procedure. First, the static potential $V^s_{nl}(r)$ corresponding to a given nl state was obtained by using the Hartree-Fock-Slater wave functions $\varphi_{n'l'}(x)$ [15] in the usual form:

$$V^s_{nl}(r) = \sum_{n'l'\neq nl} \int d\mathbf{x} \frac{|\varphi_{n'l'}(x)|^2}{|\mathbf{r}-\mathbf{x}|} - \frac{Z_T}{r}. \tag{3}$$

Next, $V^s_{nl}(r)$ was fitted as $V^s_{nl}(r) \simeq \Sigma_{j=0}^4 Z_j \exp(-\mu_j r)/r$. To initiate the fitting procedure, the Molière parameters Z_j and μ_j were used. We note in this respect that by using different starting seeds we may arrive at different sets of parameters. The sum of charges equals the target nucleus charge Z_T, i.e., $\Sigma_{j=0}^4 Z_j = Z_T$, and the first term carries the information about the asymptotic Coulomb condition, i.e., $\mu_0=0$ and $Z_0=0$, 1, and 2 for negative, neutral, and positive ions, respectively. In the next step, $V^s_{nl}(r)$ was extended to a more general form:

$$V_{nl}(r) = \frac{1}{r}\sum_{j=1} Z_j \exp(-\mu_j r)(1+\alpha_j r), \tag{4}$$

where the parameters μ_j and α_j were adjusted by solving the corresponding radial Schrödinger equation and demanding that the binding energy E_{nl}, $\langle r\rangle_{nl}$, and $\langle 1/r\rangle_{nl}$ be as close as possible to the corresponding values obtained by using the starting Hartree-Fock method. In all cases E_{nl} was obtained with at least four significant figures and $\langle 1/r\rangle_{nl}$ with a rela-

tive error less than 1%. In most cases $\langle r\rangle_{nl}$ was achieved within a relative error of less than 1%, except for the outer shells of Xe $(5p,5s)$, I^- $(5p,5s)$, and Br^- $(4p)$, in which $\langle r\rangle_{nl}$ reached relative errors of around 2%. While for positive atoms the method does not present any problems, for anions, the procedure requires a certain degree of care, especially for the outer shells.

B. Calculation of the SLPA

For the case of bare projectiles of charge Z_P colliding with a single target, the cross section in the SLPA [16,17] reads

$$\sigma_{nl}^{\mathrm{SLPA}} = \int_{\omega_m}^{\infty} d\omega \int_{\omega/v}^{\infty} dq\, W_{nl}(q,\omega), \tag{5}$$

$$W_{nl}(q,\omega) = \int d\mathbf{r} \frac{2Z_P^2}{\pi v q}\left[\frac{1}{\varepsilon[\omega_g,q,\omega,k_{Fnl}(r)]} - 1\right], \tag{6}$$

where, as usual, $k_{Fnl}(r)$ is the space-dependent Fermi velocity, $k_{Fnl}(r)=[3\pi^2\rho_{nl}(r)]^{1/3}$, $\rho_{nl}(r)$ is the electron density of the nl state $\rho_{nl}(r)=|\varphi_{nl}(r)|^2$, $\varphi_{nl}(r)$ is the bound-state wave function given the tables of Refs. [15,18]. In Eq. (6), r is the position of the projectile with respect to the target, q and ω are the momentum and energy deposited by the projectile, and $\varepsilon(\omega_g,q,\omega,k_{Fnl})$ is the dielectric response function. Note that we have explicitly denoted the lower extreme of integration of Eq. (5) by ω_m, which is the minimum energy that one electron needs to be ionized. In the traditional local plasma approximation it is set to $\omega_m=0$.

As in our previous calculation we have used the Levine-Louie dielectric response function $\varepsilon^{\mathrm{LL}}(\omega_g,q,\omega,k_{Fnl})$ [19] defined as follows:

$$\mathrm{Im}\,\varepsilon^{\mathrm{LL}}(\omega_g,q,\omega,k_{Fnl}) = \begin{cases} \mathrm{Im}\,\varepsilon^{L}(q,\tilde{\omega},k_{Fnl}), & \omega > \omega_g, \\ 0, & \omega < \omega_g, \end{cases} \tag{7}$$

where ε^L is the Lindhard dielectric function and $\varepsilon^{\mathrm{LL}}$ is a function of the energy shift $\tilde{\omega}^2=\omega^2-\omega_g^2$, with ω_g being the gap, i.e., the threshold energy. After simple algebra, a closed form for $\varepsilon^{\mathrm{LL}}(q,\omega,k_{Fnl})$ can be found (for details see Refs. [17,19]). By definition, $\varepsilon^{\mathrm{LL}}$ *does* satisfy the f-sum rules.

The f-sum rule is a closure property which relates all the possible transfer energies between ω_g and ∞. These inelastic transitions involve also all the possible excitation channels not considered here. Since our negative ions do not have excited states, the gap is certainly the ionization energy, i.e., $\omega_m=\omega_g=|E_{nl}|$, and we do not have any doubt at all. Even though we have excited states in neutral atoms, their contribution is not relevant so we can also approximate $\omega_m\cong\omega_g=|E_{nl}|$. But for positive ions we have a different situation since they present a first excited state (that is the minimum gap ω_g in our formalism) with binding energies substantially smaller than the ionization energy $\omega_m=|E_{nl}|$. Values of ω_m and ω_g used for Li^+, Na^+, K^+, and Rb^+ are given in Ref. [20].

III. RESULTS

In every case, nine proton impact energies ranging from 25 keV to 1 MeV were calculated. Ionization cross sections

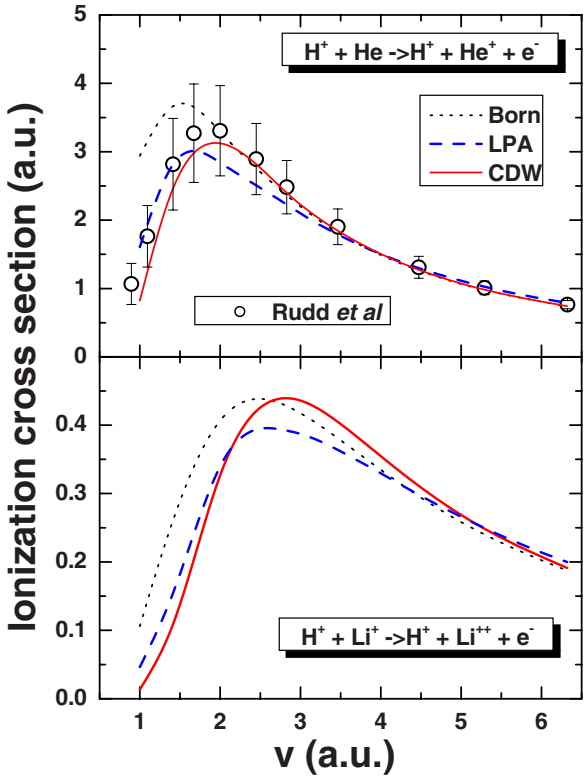

FIG. 1. (Color online) Ionization cross section for protons on He^0 and Li^+, as a function of the impact velocity. All quantities in atomic units. Empty circles, recommended experiments from Rudd *et al.* [22]. Theories: Solid (red) lines CDW-EIS, dotted (black) lines Born approximation, and dashed (blue) lines SLPA.

for the He (He^0,Li^+), Ne (F^-,Ne^0,Na^+), Ar (Cl^-,Ar^0,K^+), Kr (Br^-,Kr^0,Rb^+), and Xe (I^-,Xe^0) isoelectronic series are displayed in Figs. 1–5. We use the same notation in all the figures: CDW-EIS results are plotted with solid lines (red), Born results with dotted lines (black), and SLPA results with dashed lines (blue). Before proceeding, we want to point out a formal difference between the CDW-EIS (or Born) approximation and the SLPA. The former assumes an *independent electron* formalism while the latter is a *many-electron model*, where all the electrons of the shell are fully correlated. In addition, there is another point to be taken into consideration: the SLPA is a first-order approximation in the projectile charge while the CDW-EIS approximation includes all orders, at least approximately. In this respect the SLPA should have the same status as the first Born approximation. One would expect that in the perturbative regime both approaches should converge, at least for the stopping power where the f-sum rule dominates [21].

We start by considering the He isoelectronic series, shown in Fig. 1, where results within the CDW-EIS method were already reported by Gulyás *et al.* [8]. This case should be considered out of the scope of the SLPA since a two-electron target cannot be considered as a many-electron system. The case of H^- is excluded since it cannot be treated by the CDW-EIS approach because the independent electron model fails. A rapid convergence of the CDW-EIS result to the Born limit is observed, as well as a good performance of the SLPA (unexpected for this case). No significant differences be-

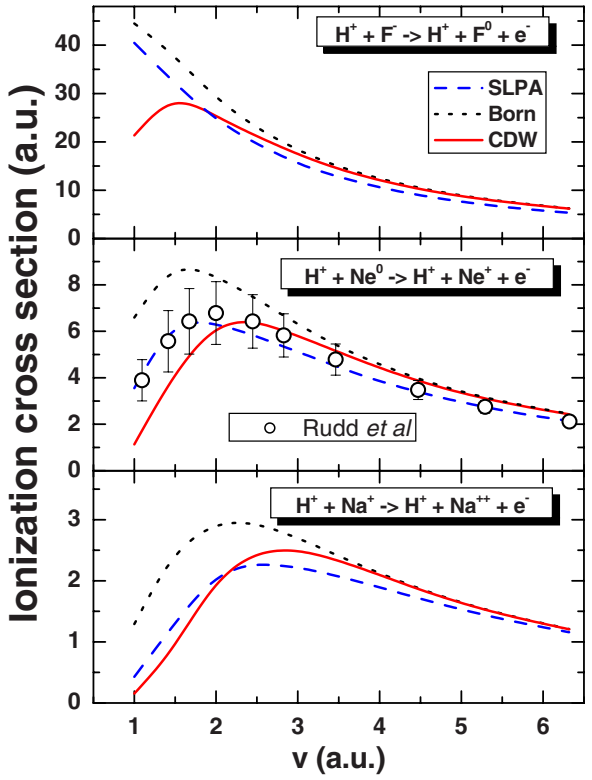

FIG. 2. (Color online) Ionization cross section for protons on F^-, Ne^0, and Na^+, as a function of the impact velocity. All quantities in atomic units. Empty circles, recommended experiments from Rudd *et al.* [22]. Theories, as indicated.

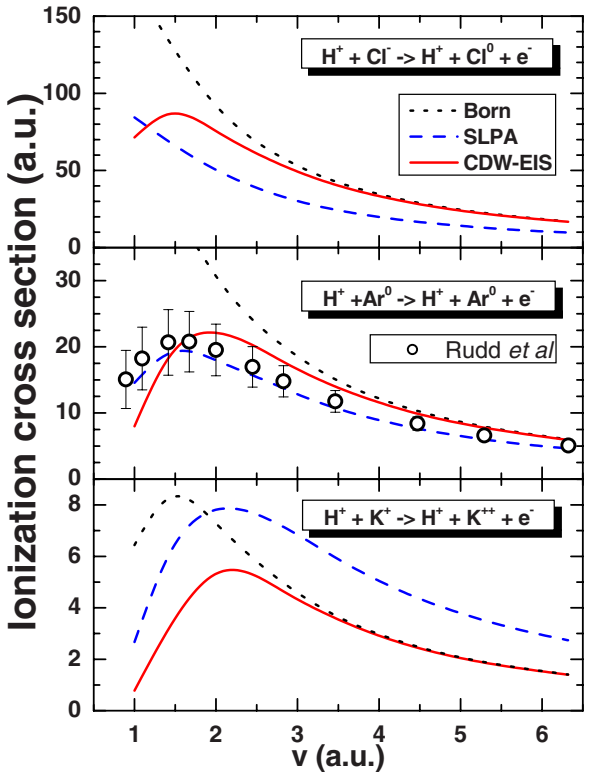

FIG. 3. (Color online) Ionization cross sections for protons on Cl^-, Ar^0, and K^+, as a function of the impact velocity. All quantities in atomic units. Empty circles, recommended experiments from Rudd *et al.* [22]. Theories, as indicated.

tween previous calculations [8] and ours are observed in the considered range of energies. For the helium target, we also show the recommended values published by Rudd and co-workers [22] obtained after fitting a series of experiments. According to Table III of that publication, experimental errors vary between 10% in the high energy to 25% for the lower energies. All the approximations reproduce these experimental values neatly, running close to each other.

The cross sections for the Ne isoelectronic series are presented in Fig. 2 along with the recommended values of Rudd and collaborators for Ne [22]. In the high-energy range our CDW-EIS results run about 13% above the ones reported by Gulyás *et al.* [8], which are close to the experimental results of Rudd *et al.* In addition to numerical uncertainties, the difference between the two theoretical results should be attributed only to the different potential employed. The CDW-EIS values converge quite well to the Born ones for impact energies larger than 300 keV. In all the cases the SLPA gives a very good description of the CDW-EIS results for the ions and also for the experiments with neutral targets.

Ionization cross sections for the Ar isoelectronic series are shown in Fig. 3 as a function of the proton velocity. The flag target in this isoelectronic set is Ar, for which a set of experiments were carried out. In the figure, we show again the experimental values fitted by Rudd and co-workers [22]. Errors vary between 10% at high energy and 25% near the maximum of the cross section. At high energies, our CDW-EIS results run about 15% above the experiments but close to the results of Gulyás *et al.* [8]. Our high-energy limit seems again to be slightly larger than the experimental values. CDW-EIS results tend to the Born approximation for energies higher than 300 keV and the SLPA gives a good description of the experiments for neutral Ar. For this system we start to observe a pathology of singly charged ions that will persist in the following series under study: the SLPA overestimates the results for the K^+ target, while on the contrary it underestimates the cross section for Cl^-. Next we discuss the possible origins of these discrepancies. To avoid any kind of doubt in this respect, we also evaluate the first Born approximation with $l_{max}=32$, and no observable difference was found.

We have calculated the ionization of the L shell of Ar and reproduced the CDW-EIS results of Ref. [8] and the experiments within less than 10%. Therefore, one can conclude that the CDW-EIS method works very well for ionization of inner shells and therefore, by similarity of the target, it should work also for ionization of positive ions. So we should argue that the SLPA overestimates the ionization cross section for this case. One possible failure is that the prescription we use to extract the excitation contribution between $|E_{4s}|=\omega_g$ and the ionization threshold $|E_{3p}|=\omega_m$, which totals only 15% in the high-energy limit, is insufficient. Another source of failure may be the fact that the Coulomb core K^{2+} produces a strong variation of the electron density to the point that the local approximation fails.

The situation is different for Cl^-, because we do not have excited states and there is no doubt that $\omega_m=\omega_g=|E_{3p}|$. Further, the outer shell of Cl^- is a good candidate to be modeled

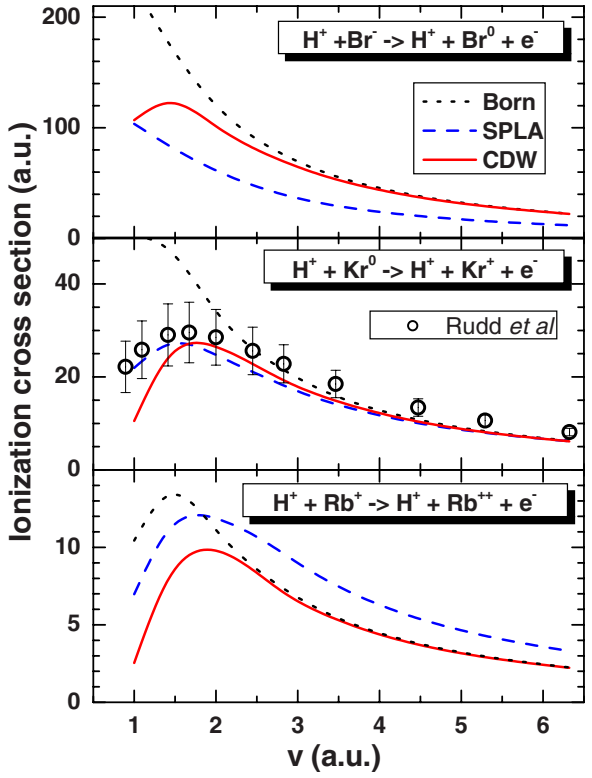

FIG. 4. (Color online) Ionization cross sections for protons on Br^-, Kr^0, and Rb^+, as a function of the impact velocity. All quantities in atomic units. Empty circles, recommended experiments from Rudd *et al.* [22]. Theories, as indicated.

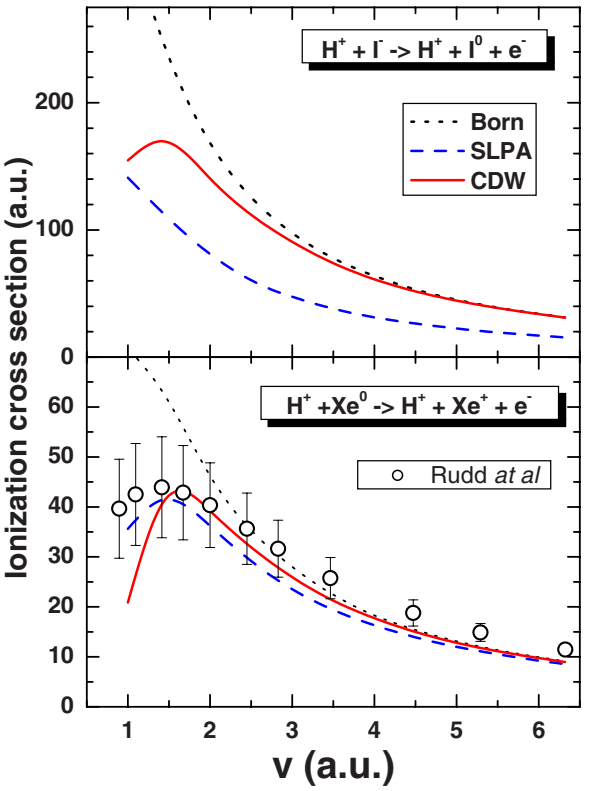

FIG. 5. (Color online) Ionization cross sections for protons on I^- and Xe^0, as a function of the impact velocity. All quantities in atomic units. Empty circles, recommended experiments from Rudd *et al.* [22]. Theories, as indicated.

with a free electron gas. To explain the observed discrepancy, we put forward the possibility that all the electrons of the outer shell of Cl^- *do* shield the projectile and therefore diminish the electron production of low energies and consequently the cross section. This effect is not taken into account by the CDW-EIS, which is based in the independent electron model, but it is included in the SLPA because it is a many-electron model. No effect should be observed for high-energy electrons coming from small electron-projectile distances, and so the SLPA should provide a good description of the stopping power. It would be interesting to elucidate experimentally if this consideration is true.

Results for the Kr isoelectronic series are shown in Fig. 4. The reference target of this set is Kr and, to our knowledge, there are no reported CDW-EIS values to compare with. Recommended values of Rudd and co-workers [22] are included in the figure. Fitting errors vary between 10% and 25%. Our theory overestimates the experimental fitting by 25% at 1 MeV. In any case, fitting values may be rather large by about 24% in comparison with the corresponding optical values (see Ref. [22], p. 988). CDW-EIS values converge very rapidly to the Born approximation. The SLPA gives a very good description of the experiments at intermediate energies and converge to the Born limit in the perturbative regime. The same pathology is observed for the singly charged ions; the SLPA overestimates the results for Rb^+ target, while, on the contrary, it underestimates the cross section for Br^-.

Finally, in Fig. 5 we present calculated cross sections for Xe and I^-. Recommended values for Xe target reported by Rudd and co–workers are included again in the figure [21]. Very few experiments were available to be fitted and the uncertainty errors were estimated to vary between 10 and 25%. Our high-energy limit value runs 20% above the fitted experimental value in the high-energy limit. The same behaviors are observed: a rapid convergence to the Born approximation, a good performance of the SLPA, and an underestimation for negative ions of the SLPA in comparison with the CDW-EIS theory.

As mentioned in the Introduction, several CDW-EIS calculations have been simplified by employing an effective Coulomb charge to represent the continuum, i.e., $Z_{\text{eff}} = \sqrt{2|E_{nl}|}$. Using Hartree-Fock-Slater orbitals to represent the initial bound state, closed forms can be achieved for the T matrix, which makes the calculation very fast. To quantify the differences, in Fig. 6 we plot the ratio $\epsilon_{\text{eff}} = [\sigma(Z_{\text{eff}}) - \sigma]/\sigma$, where $\sigma(Z_{\text{eff}})$ is the ionization cross section using Z_{eff} and σ represents our ionization results as shown in Figs. 1–5. It is difficult to find a systematic trend for ϵ_{eff}. One may generalize by stating that the more loosely bound the outer electrons the larger the spread of ϵ_{eff}. The errors ϵ_{eff} are quite noticeable at intermediate energies and decrease as the impact velocities increase, although they do not necessarily vanish in the high-velocity limit. At high impact energies, say 1 MeV, errors vary from −40% (for I^-) to +50% for F^-, showing lower values for positive ions.

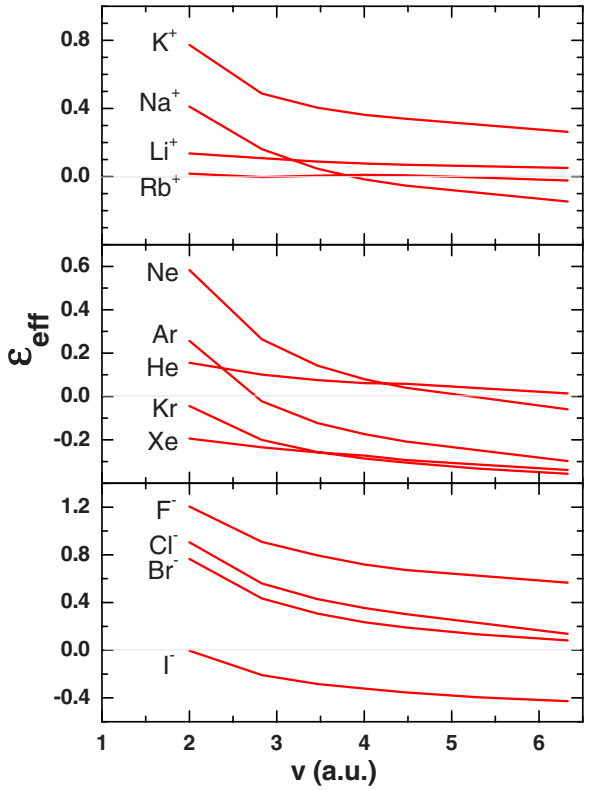

FIG. 6. (Color online) Relative errors of the CDW $\epsilon_{\text{eff}} = [\sigma(Z_{\text{eff}}) - \sigma]/\sigma$, where $\sigma(Z_{\text{eff}})$ is the ionization cross section using Z_{eff} in the Coulomb final state and σ represents our ionization results shown in the previous figures.

IV. CONCLUSIONS

We have obtained a series of results which are of great interest for collision with ClNa insulators, and also for collisions with ionized gases. We have reported total ionization cross sections for protons colliding with targets of the He, Ne, Ar, Kr, and Xe isoelectronic series involving neutral, positive, and negative singly-charged ions in a systematic and complete way. The central potentials were determined from the Hartree-Fock wave functions and improved to achieve the best binding energies and moments of the position (E_{nl}, $\langle r \rangle_{nl}$, and $\langle 1/r \rangle_{nl}$). Calculations were carried out with the CDW-EIS and first-order Born approximations, to the best of present computational abilities. This demanded a considerable computational effort. To our knowledge, this is the first time that the full CDW-EIS method has been used to calculate the singly charged isoelectronic series, and for Kr and Xe rare gases. To shed light on previous calculations of electron yields of proton on insulators, we compared the prediction of the SLPA against the CDW-EIS method and with the available experiments on rare gases.

Let us summarize the four main conclusions of this work.

(i) In all cases the Born approximation rapidly tends to the CDW-EIS results. It could save a huge amount of computational time if we focus on impact energies larger than 300 keV.

(ii) Our high-energy limits run 25 and 20% below the recommended experimental values for Kr and Xe, and 13 and 15% above for Ne and Ar, respectively.

(iii) For total cross sections, the SLPA gives a good account of the CDW-EIS results for neutral atoms, and both theories provide a very good description of the experiments.

(iv) For the Ar, Kr, and Xe isoelectronic series, the SLPA overestimates (underestimates) the CDW-EIS results for positive (negative) ions.

We call on experimentalists to measure collisions with single negative ions since it could elucidate the role of the multielectron screening effect due to the outer shells. This effect is neglected in the independent electron model and partially included in the SLPA. We intend to proceed with the calculation of stopping and straggling for the present series.

ACKNOWLEDGMENTS

The authors would like to acknowledge financial support from CONICET, UBACyT, and ANPCyT of Argentina. We wish to thank F. Salvat for providing us the latest version of the program RADIALF.

[1] For a comprehensive review, see H. Winter, Phys. Rep. **367**, 387 (2002).
[2] K. Kimura, G. Andou, and K. Nakajima, Phys. Rev. Lett. **81**, 5438 (1998).
[3] G. Andou, K. Nakajima, and K. Kimura, Nucl. Instrum. Methods Phys. Res. B **160**, 16 (2000).
[4] A. J. García and J. E. Miraglia, Phys. Rev. A **74**, 012902 (2006); **75**, 042904 (2007).
[5] A. García and J. E. Miraglia (unpublished).
[6] M. S. Gravielle, I. Aldazabal, A. Arnau, V. H. Ponce, J. E. Miraglia, F. Aumayr, S. Lederer, and H. Winter, Phys. Rev. A **76**, 012904 (2007).
[7] P. D. Fainstein, R. Rivarola, and V. H. Ponce, J. Phys. B **21**, 287 (1988), and references therein.
[8] L. Gulyás, P. D. Fainstein, and A. Salin, J. Phys. B **28**, 245 (1995).
[9] L. Gulyás and T. Kirchner, Phys. Rev. A **70**, 022704 (2004).
[10] P. D. Fainstein, L. Gulyás, and A. Dubois, J. Phys. B **31**, L171 (1998).
[11] L. Gulyás and P. D. Fainstein, J. Phys. B **31**, 3297 (1998).
[12] S. Manson, L. H. Toburen, D. H. Madison, and N. Stotelfoht, Phys. Rev. A **12**, 60 (1975).
[13] A. R. Edmonds, *Angular Momentum in Quantum Mechanics* (Princeton University Press, Princeton, NJ, 1968), Eq. (5.7.2).
[14] F. Salvat, J. M. Fernández-Varea, and W. Williamson, Jr., Comput. Phys. Commun. **90**, 151 (1995).
[15] E. Clementi and C. Roetti, At. Data Nucl. Data Tables **14**, 177 (1974).
[16] C. C. Montanari, J. E. Miraglia, M. Behar, P. F. Duarte, N. R. Arista, J. C. Eckardt, and G. H. Lantschner, Phys. Rev. A **77**,

042901 (2008).
[17] C. D. Archubi, C. C. Montanari, and J. E. Miraglia, J. Phys. B **40**, 943 (2007).
[18] C. F. Bunge, J. A. Barrientos, and A. V. Bunge, At. Data Nucl. Data Tables **53**, 113 (1993).
[19] Z. H. Levine and S. G. Louie, Phys. Rev. B **25**, 6310 (1982).
[20] For Li^+, we have $\omega_m=|E_{1s}|=2.792$, and using the potential V_{1s}, the first excited state was calculated to be $E_{2p}=-0.5116$, so in Eq. (8) we have used $\omega_g=|E_{2p}|$. Similarly for Na^+, we have $\omega_m=|E_{2p}|=1.797$, and using V_{2p}, we obtain $|E_{3s}|=0.5306=\omega_g$. For K^+, $\omega_m=|E_{3p}|=1.171$, and using V_{3p}, we obtain $|E_{4s}|=0.4233=\omega_g$; and for Rb^+, $\omega_m=|E_{4p}|=1.098$, and using V_{4p}, we obtain $|E_{5s}|=-0.3988=\omega_g$.
[21] W. K. Chu and D. Powers, Phys. Lett. **40A**, 23 (1972).
[22] M. E. Rudd, Y.-K. Kim, D. H. Madison, and J. W. Gallagher, Rev. Mod. Phys. **57**, 965 (1985).